Nucleation in *A*/*B*/*AB* blends: Interplay between microphase assembly and macrophase separation

Jiafang Wang,[1,2,a)] Marcus Müller,[2] and Zhen-Gang Wang[3]
[1]*State Key Laboratory of Polymer Physics and Chemistry, Changchun Institute of Applied Chemistry, Chinese Academy of Sciences, Changchun 130022, People's Republic of China*
[2]*Institut für Theoretische Physik, Georg-August Universität, D-37077 Göttingen, Germany*
[3]*Division of Chemistry and Chemical Engineering, California Institute of Technology, Pasadena, California 91125, USA*

(Received 19 January 2009; accepted 24 February 2009; published online 20 April 2009)

We study the interplay between microphase assembly and macrophase separation in *A*/*B*/*AB* ternary polymer blends by examining the free energy of localized fluctuation structures (micelles or droplets), with emphasis on the thermodynamic relationship between swollen micelles (microemulsion) and the macrophase-separated state, using self-consistent field theory and an extended capillary model. Upon introducing homopolymer *B* into a micelle-forming binary polymer blend *A*/*AB*, micelles can be swollen by *B*. A small amount of component *B* (below the *A*-rich binodal of macrophase coexistence) will not affect the stability of the swollen micelles. A large excess of homopolymer, *B*, will induce a microemulsion failure and lead to a macrophase separation. Between the binodal and the microemulsion failure concentration, macrophase separation in *A*/*B*/*AB* occurs by a two-step nucleation mechanism via a metastable microemulsion droplet of finite size. Our results illustrate a recently proposed argument that the two-step nucleation via a metastable intermediate is a general phenomenon in systems involving short-range attraction and long-range repulsion. © *2009 American Institute of Physics*. [DOI: 10.1063/1.3105340]

I. INTRODUCTION

Highly immiscible *A*/*B* mixtures with an amphiphilic compound *CD* are of great interest due to their rich phase behaviors and extensive applications.[1–28] The amphiphilic molecule *CD* has two parts connected by a chemical bond, such that part *C* likes *B* and part *D* likes *A*. Therefore, adding *CD* to *A*/*B* mixtures may improve their miscibility and even prevent macrophase separation, or lead to the formation of structures with a characteristic length scale set by the molecular extension. One well-known example is water/oil/surfactant mixture, which may form oil-in-water, water-in-oil, or bicontinuous microemulsions.[1–4] These microemulsions have been used *inter alia* in drug delivery, oil recovery, reaction vessel applications. A diblock copolymer *CD* is the polymeric counterpart of an amphiphilic surfactant. Diblock copolymers, *CD*, are comprised of a *C*-block and a *D*-block. The immiscibility between the long, flexible *C*- and *D*-blocks leads to microscopic phase separation and periodically ordered structures are created.[29–32] When a diblock copolymer, *CD*, is mixed with two incompatible homopolymers, *A*/*B*, or solvents of low molecular weight, which are selective for the two blocks, respectively, the interplay between microphase and macrophase separation gives rise to a complex phase behavior.[5–28,33] If only a small amount of homopolymers, *A*/*B*, is added, microscopic phase separation will still occur, and the ordered structures of block copolymer, *CD*, will be swollen by the homopolymers, *A* and *B*. When the amount of homopolymers increases further (close to the concentration, where mean-field-theory predicts a Lifshitz point), unbinding transitions destroy the long-range order of periodic structures, resulting in locally assembled structures without the long-range order, such as spherical micelles, wormlike micelles, or microemulsions.[12–28,33] If the amount of diblock copolymer further decreases, the locally assembled structures will become unstable, and the system undergoes macroscopic phase separation into *A*-rich and *B*-rich phases. One prominent example is the emulsion failure that occurs when one increases the amount of homopolymer, *B*, or decreases the amount of diblock copolymer, *CD*, in the micelle-forming system of *A*/*B*/*CD* blends.[28] Even in this simple system, it is not clear whether the transition from the microemulsion to macrophase separation occurs spontaneously or via nucleation and growth mechanism. The behavior of the ternary system, *A*/*B*/*CD*, however, is even more complex because there are multiple two-phase and three-phase coexistences. In this work, we study the mechanism of phase transformation by studying the nucleation in *A*/*B*/*CD* systems, with a focus on the interplay between swollen micelles and macrophase separation.

Effects of diblock copolymer *AB* on the nucleation of an *A*/*B* blend have been studied theoretically[34] and experimentally,[35,36] without explicitly considering the interference of micelle formation. In previous work,[34] we have studied effects of adding diblock copolymers, *AB*, on the nucleation in the course of macrophase separation in an *A*/*B* blend at weak segregation ($\chi N \approx 3$). It has been shown that adding diblock copolymer, *AB*, to the *A*/*B* blend can either increase or decrease the nucleation free energy barrier rela-

a)Electronic mail: wang@theorie.physik.uni-goettingen.de.

tive to the pure A/B blend. The qualitative trend can be deduced from the shift of the coexistence boundary (i.e., binodal) and the spinodal. Balsara and coworkers[35,36] observed that an increase in the amount of diblock copolymers can either switch the mechanism of phase separation from spinodal decomposition to nucleation or decrease the rate of nucleation. In the strong segregation regime, however, the block copolymers are more likely to form micelles. Therefore the question arises as to how these micelles affect the kinetics of macrophase separation. It is well known that micelles are formed in A/CD blends or asymmetric block copolymer melts by a nucleation mechanism and that micelles correspond to a local minimum of the excess free energy.[37–42] However, the relationship between the nucleation of micelle formation and the mechanism of macrophase separation has not been elucidated. Recently, Hutchens and Wang[43] showed that in solutions of charged particles, a bulk condensation transition can occur by a two-step nucleation mechanism with a metastable liquid cluster intermediate of finite size. The authors suggested that this two-step nucleation scheme is a common feature of systems with short-range attraction and long-range repulsion. Since, phenomenologically, the diblock copolymer homopolymer mixture can be mapped onto a system with short-ranged attraction and screened Coulomb repulsion,[10,29,30,44] we conjecture that a two-step nucleation for macrophase separation should also be observed in $A/B/CD$ blends and that the metastable intermediate of finite size is a swollen micelle.

In this paper, we use two complementary theoretical methods to investigate the nucleation in $A/B/AB$ ternary blends, which is a special case of the more general $A/B/CD$ mixtures. On the one hand we use numerical self-consistent field theory (SCFT). SCFT has been successfully extended to study local self-assembled structures such as micelles, emulsion droplets and critical nuclei of macrophase separation.[34,41,45–48] Using the SCFT method, we can calculate the density profiles and free energy of localized fluctuation structures (e.g., micelles or nuclei/droplets of the new, stable phase during phase transformation) at the mean-field level without further approximation. Additionally, we employ a combination of capillary model and diblock copolymer monolayer model. This method is based on the assumption that homopolymers, B, constitute the core of the nucleus and diblocks, AB, form a monolayer at the interface of A/B. The free energy of the diblock copolymer monolayer is considered using a dry brush model. Assuming the structure of the fluctuation, we can straightforwardly calculate the free energy excess in the two-dimensional parameter space spanned by the material excess of B and AB.

The remainder of the paper is organized as follows: In Sec. II, we briefly describe the SCFT and its numerical application to the calculation of critical nuclei for the general case of $A/B/CD$ ternary systems. The main results, which are restricted to the $A/B/AB$ blends, are presented in Sec. III. We first discuss the results from numerical self-consistent field calculations and, then, present an extended capillary model. We conclude in Sec. IV with a summary of the main results.

II. NUMERICAL SELF-CONSISTENT FIELD THEORY

In the following, we briefly present the SCFT of an incompressible ternary blend consisting of homopolymers, A and B, and a diblock copolymer, CD, with degrees of polymerization N_α (where the subscript α denotes chain species, i.e. $\alpha=A,B,CD$). The fraction of C-block of the diblock copolymer CD is f. All polymers are assumed to be flexible and modeled as Gaussian chains. For simplicity, we assume identical monomeric volumes, v, and Kuhn lengths, b, for all polymer species. In order to study nucleation and micelle formation in a metastable bulk (denoted as mother phase in the following), it is convenient to work in the (semi-) grand canonical ensemble controlling the chemical potentials μ_α^b. Because not all chemical potentials of the components in an incompressible mixture are independent, we set $\mu_{CD}^b=0$. The derivation of the SCFT is similar to that in Refs. 11 and 12 and only the salient features are summarized. The grand potential of the ternary blend in a volume, V, can be written as

$$G=-\sum_\alpha \frac{\exp(N_\alpha v\mu_\alpha^b)}{N_\alpha v}Q_\alpha[\{\omega_j\}] + \int_V d^3r\left[\frac{1}{2}\sum_{jj'}\frac{\chi_{jj'}}{v}\phi_j(r)\phi_{j'}(r)-\sum_j \omega_j(r)\phi_j(r)+\xi(r)\times\left(\sum_j \phi_j(r)-1\right)\right], \tag{1}$$

where G, $\chi_{jj'}$, ω_j, ξ, and μ_α^b have been scaled by k_BT. The subscripts j and j' denote monomer species, i.e., $j(j')=A,B,C,D$. $\chi_{jj'}$ is the Flory–Huggins interaction parameter between monomer j and j' and $\chi_{jj}=0$. ϕ_j is the volume fraction of monomer j, and ω_j is the self-consistent, molecular field conjugated to ϕ_j, and ξ denotes the effective pressure field that enforces the incompressibility constraint.

In Eq. (1), Q_α denotes the single chain partition function of a chain, α, in the presence of external fields, $\{\omega_j\}$,

$$Q_\alpha[\{\omega_j\}]=\int_V d^3r q_\alpha(r,N_\alpha), \tag{2}$$

where the end-segment distribution function, $q_\alpha(r,N_\alpha)$, is obtained from solving the modified diffusion equation

$$\left[\frac{\partial}{\partial s}-\frac{b^2}{6}\nabla_r^2+v\omega_\alpha(r)\right]q_\alpha(r,s)=0, \tag{3}$$

with α for homopolymers, A and B, and

$$\left[\frac{\partial}{\partial s}-\frac{b^2}{6}\nabla_r^2+v\omega_C(r)\right]q_{CD}(r,s)=0;\quad s\in[0,fN_{CD}],$$

$$\left[\frac{\partial}{\partial s}-\frac{b^2}{6}\nabla_r^2+v\omega_D(r)\right]q_{CD}(r,s)=0;\quad s\in[fN_{CD},N_{CD}] \tag{4}$$

for the diblock copolymer CD. The initial conditions for the diffusion equations are $q_\alpha(r,0)=1$. Because of the lack of inversion symmetry of diblock copolymer, CD, it is necessary to introduce a conjugate end-segment distribution,

$q^{\dagger}_{CD}(r,s)$, which satisfies a similar modified diffusion equation as Eq. (4) with $\partial/\partial s$ multiplied by -1 and initial condition $q^{\dagger}_{CD}(r,N_{CD})=1$.

The self-consistent field equations are obtained by a variational extremization of the grand potential with respect to $\{\omega_j\}$ and $\{\phi_j\}$, respectively, in conjunction with the incompressibility constraint $\Sigma_j \phi_j = 1$. This procedure yields

$$\phi_C = \frac{1}{N_{CD}} \int_0^{fN_{CD}} ds q_{CD}(r,s) q^{\dagger}_{CD}(r,s),$$

$$\phi_D = \frac{1}{N_{CD}} \int_{fN_{CD}}^{N_{CD}} ds q_{CD}(r,s) q^{\dagger}_{CD}(r,s),$$

$$\phi_A = \frac{\exp(N_A v \mu^b_A)}{N_A} \int_0^{N_A} ds q_A(r,s) q_A(r,N_A - s),$$

$$\phi_B = \frac{\exp(N_B v \mu^b_B)}{N_B} \int_0^{N_B} ds q_B(r,s) q_B(r,N_B - s),$$

$$v\omega_j = \sum_{j'} \chi_{jj'} \phi_{j'} + v\xi, \quad j{:}A,B,C,D. \tag{5}$$

From the self-consistent field equations, we can determine the stationary points in the grand potential surface, including the local minima and saddle points corresponding to micelles and critical nuclei, respectively. Using the solutions to the self-consistent field equations, we can rewrite the grand potential as

$$G = -\sum_{\alpha} \frac{\exp(N_\alpha v \mu^b_\alpha)}{N_\alpha v} Q_\alpha[\{\omega_j\}] - \int_V d^3 r \left[\xi(r) + \frac{1}{2} \sum_{jj'} \frac{\chi_{jj'}}{v} \phi_j(r) \phi_{j'}(r) \right]. \tag{6}$$

The homogeneous bulk (mother phase) is always a solution to the self-consistent field equations, which is given in the Appendix. There, we also sketch the location of the coexistence and the spinodal for macrophase separation into A-rich and B-rich coexistent phases in an $A/B/CD$ ternary blend.

For the localized fluctuation structures (e.g., micelles or droplets), the self-consistent field equations need to be solved numerically to obtain the solution $\{\phi_j\}$, $\{\omega_j\}$, and ξ for a spatially inhomogeneous system. We consider the excess free energy of creating a single, localized fluctuation structure in the mother phase.[34,41,45,46,49] The mother phase is characterized by the chemical potentials. The basic idea is to focus on an appropriately chosen volume in a large system and ask what the free energy cost is for creating a specified type of fluctuation with its center-of-mass position fixed at the center of the volume (i.e., the translational entropy of the single, localized fluctuation structure is not considered). The computational cell is chosen large enough for the localized fluctuation structure to decay at the boundary at the computational cell, where the mother phase is recovered. In the (semi-) grand canonical ensemble the fluctuation and the mother phase can exchange particles. In the following, we restrict ourselves to spherically symmetric fluctuation structures. Therefore, we solve the self-consistent field equation in a spherical coordinate system, only considering a spatial variation in the radial direction. Deviations from the spherical symmetry may lower barriers, but it is out of the scope of this paper. We constrain the size of the fluctuation structure by requiring that the volume fraction of a given component adopts a specified value on a shell of radius, R. The quantity, R, acts as a reaction coordinate that parameterizes the evolution of the fluctuation structure (and the process of phase transformation). The free energy functional of the SCFT is extremized under this local, crossing constraint. The concomitant Lagrange field, which enforces this constraint, acts on the shell of radius, R.[46] If the Lagrange field vanishes, the localized fluctuation structure is an extremum of the unconstraint system, i.e., a (meta-) stable micelle or the critical nucleus.

From the solution, $\{\phi_j\}$, $\{\omega_j\}$ and ξ, the grand potential of the localized fluctuation structure, $G[\{\phi_j\},\{\omega_j\},\xi]$, can be calculated according to Eq. (6). Usually, the excess free energy or work of formation of the localized fluctuation structure is more useful. Subtracting the grand potential of the uniform phase $G[\{\phi^b_j\},\{\omega^b_j\},\xi^b]$ from that of the localized fluctuation structure, we obtain the reversible excess free energy of formation as

$$\Delta G = G[\{\phi_j\},\{\omega_j\},\xi] - G[\{\phi^b_j\},\{\omega^b_j\},\xi^b]. \tag{7}$$

To quantify the size of the fluctuation structure, we use the "material excess," which is defined as $M \equiv \int_V d^3 r [\phi^b_A - \phi_A(r)]$. Note that in our calculation, we specify the chemical potential of the species in the mother phase and the reaction coordinate, R. If we used, instead, the material excess as reaction coordinate (integral criterion), the corresponding Lagrange field would be the bulk chemical potential, μ^b_A. In the case of an integral criterion, we would be considering (meta-) stable micelles or critical nuclei of different material excess in *different* mother phases, rather than calculating the growth of a micelle or nucleus in a given mother phase.

We calculate the excess free energy of the localized fluctuation structure and study its dependence on the measured material excess, i.e. $\Delta G(M)$. From this information, we can identify the critical nucleus as local maxima and micelles or microemulsion droplets as local minima, as will be discussed later.

III. RESULTS AND DISCUSSION

A. Results of SCFT calculation

A general $A/B/CD$ ternary blend involves a large number of parameters.[13–19] As the first step, we study a simple case, $A/B/AB$, and assume all polymer species have equal degree of polymerization, i.e. $N_A = N_B = N_{AB} = N$. Therefore the system is specified by $\chi N \equiv \chi_{AB} N$, ϕ^b_{AB}, f, and ϕ^b_B. For all the results we present here, the asymmetry of the diblock is set to $f=0.67$ and the incompatibility is $\chi N = 20$. Under this condition, numerical SCFT calculations show that micelles are a local minimum of the excess free energy for ϕ^b_{AB}

$> \phi_{AB}^{md}=0.0486$. We do not expect qualitatively different effects for alternative values of f and χN, where micelles can form.

To make results applicable for general N, it is instructive to use dimensionless characteristics. To this end, we measure all distance in units of the mean-squared end-to-end distance, $R_e=b\sqrt{N}$ and use the invariant degree of polymerization, $\bar{\mathcal{N}} \equiv (R_e^3/vN)^2=b^6N/v^2$. The rescaled radius, $\tilde{r}$, material excess, $\tilde{M}$, grand potential per chain, $\tilde{g}$, and excess free energy, $\Delta\tilde{G}$ are defined by

$$\tilde{r} \equiv \frac{r}{R_e},$$

$$\tilde{M} \equiv \frac{M}{R_e^3},$$

$$\tilde{g} \equiv Nvg = \frac{R_e^3}{\sqrt{\bar{\mathcal{N}}}}g, \tag{8}$$

$$\Delta\tilde{G} \equiv \frac{\Delta G}{\sqrt{\bar{\mathcal{N}}}}.$$

Before going into the details of nucleation in a micelle-forming $A/B/AB$ blend, we consider two limiting cases: the nucleation to macrophase separation in an A/B binary blend ($\phi_{AB}^b=0$) and the micelle formation in an A/AB blend ($\phi_B^b=0$). Both two cases have been studied before,[40,45] and here we only briefly summarize their main features. The nucleation in an A/B binary blend leads to macrophase separation, and it occurs in the metastable region between the binodal of the phase coexistence and the spinodal. When increasing the immiscibility, χN, or increasing the volume fraction of homopolymer B, ϕ_B^b, in the mother phase, i.e., supersaturation, the free energy barrier of nucleation in A/B decreases monotonically from infinity at the binodal to zero at the spinodal. Correspondingly, in the vicinity of the binodal, the interface of critical nucleus resembles the planar interface between the coexisting phases in the bulk; but it becomes diffusive when approaching the spinodal. Therefore, nucleation in an A/B blend requires infinitely large critical nuclei at both the binodal and the spinodal.

Nucleation in an A/AB blend is different from that in an A/B binary blend in several aspects. In the metastable region, the nucleation in A/AB is similar to that in an A/B homopolymer blend except that for the former, both the excess free energy and the size of critical nucleus at the binodal (of macrophase separation into A-rich and AB-rich phases) are finite, rather than divergent as for the nucleation in A/B. Nucleation in the A/AB mixture also leads to macrophase separation, and the free energy barrier decreases to zero and the critical nucleus becomes diffusive and grows to infinity when approaching the spinodal. What is different in the A/AB mixture is that nuclei exist beyond the binodal in the single-phase region in form of the metastable localized fluctuation structure (i.e., micelles), which are local minima of the excess free energy. A micelle dissociation condition (*mdt* for temperature or *mdc* for concentration) can be identified as

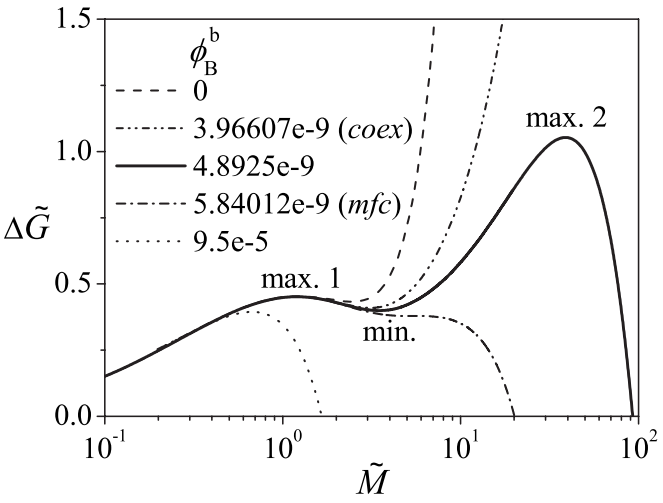

FIG. 1. Variations of the excess free energy along the path of nucleus formation at different bulk compositions of homopolymer B (ϕ_B^b) and a fixed volume fraction of block copolymer AB ($\phi_{AB}^b=0.05$), $\chi N=20$, and $f=0.67$. *mfc* ϕ_B^{mf} is defined as the concentration where the second critical nucleus disappears. It is shown that at $\phi_B^{co}<\phi_B^b<\phi_B^{mf}$, the swollen micelle is an intermediate to macrophase separation, and in this case, the first maximum is identified as the first critical nucleus (max 1), and the local minimum is swollen micelle (min) and the second maximum is the second critical nucleus (max 2).

the condition where the local minimum of ΔG (micelle) and the local maximum of ΔG (critical nucleus) merge into an inflexion point. Above *mdt* or below *mdc*, the homogeneous mother phase is absolutely stable, and no micelle with a finite lifetime exists. Usually, the formation of micelles is a microstructural assembly.[41] Therefore, it is natural to ask what is the consequence of the interplay between macrophase separation in A/B and microstructural assembly in A/AB in the ternary blend, $A/B/AB$.

The full phase behavior of $A/B/AB$ blends is very rich: $A/B/AB$ blends can exhibit macrophase separation and microphase separation and have multiple biphase coexistences, triphase coexistences, and also can from microemulsions. Here, we restrict our study to a parameter regime where the $A/B/AB$ blend only separates into macroscopically homogeneous, A-rich and B-rich coexisting phases. Micelles may form only if the temperature or concentration satisfies the *mdt* or *mdc* condition. For a melt of pure block copolymer, the *mdt* is only slightly higher than the order-disorder transition (ODT).[41] Qualitatively, introducing A and B of the same chain length into the AB diblock copolymer melts, we increase the *mdt* because the stronger incompatibility between AB block copolymer and A or B homopolymer will enhance the aggregation and assembly of AB block copolymer. Typically, however, the *mdt* still is much lower than the critical temperature of an A/B blend [corresponding to $(\chi N)_{crit}=2$] in order to drive the self-assembly of block copolymer AB. In our previous study, we have studied the nucleation in an $A/B/AB$ blend at $\chi N \approx 3$, where macrophase separation occurs without interference of metastable micelles.[34] Here, we study an $A/B/AB$ blend at a much low temperature, $\chi N=20$, to examine how micelle formation affects nucleation in $A/B/AB$ blends. We focus our discussion on the case of fixed diblock copolymer concentration while increasing the vol-

ume fraction of homopolymer B. In the last part of this section, we also consider the effects of changing the concentration of the diblock copolymer and discus a portion of the global phase diagram.

Figure 1 shows typical variations of the excess free energy of localized fluctuation structures at different values of ϕ_B^b at fixed $\chi N=20$ and $\phi_{AB}^b=0.05$. At this incompatibility, an A/AB binary blend has the *mdc* of $\phi_{AB}^{md}=0.0486$. Therefore, in the blend A/AB with $\phi_{AB}^b=0.05$, micelles will appear corresponding to a local minimum in Fig. 1 (see the dashed curve). Introducing homopolymer B into the micelle-forming A/AB blend, B will be enriched in the core of the micelle due to the strong repulsion between A and B. Then, one of two possibilities can occur: swelling of micelles (hereafter, the swollen micelles are also called microemulsions) or macroscopic phase separation into homogeneous, coexisting A-rich and B-rich phases. For an $A/B/AB$ ternary blend at $\chi N=20$, $f=0.67$, and $\phi_{AB}^b=0.05$, the coexistence density of B in the A-rich phase is $\phi_B^{co}=3.966\,07\times10^{-9}$ and the spinodal is located at $\phi_B^{sp}=0.020\,96$. When $\phi_B^b<\phi_B^{co}$, e.g., $\phi_B^b=0$, the blend is in the single-phase region so no macrophase separation is possible, and the fluctuation structure exhibits the salient feature of micelle formation. Micelles form in the uniform mother phase by overcoming a finite free energy barrier. Their growth is limited by an unbound increase in the free energy with the micelle size which characterizes the one-phase region. Adding a small amount of homopolymer, B, only leads to slight swelling of the micelles. The amount of homopolymer B in the swollen micelle increases with ϕ_B^b. When ϕ_B^b exceeds the spinodal, ϕ_B^{sp}, macrophase separation occurs spontaneously without any free energy barrier. When the blend is in the metastable region but close to the spinodal, e.g., $\phi_B^b=9.5\times10^{-5}$, the behavior typical for (one-step) nucleation to macrophase separation occurs, which is similar to the phase transformation in A/B and A/AB blends.

Interestingly, we observe that, when ϕ_B^b is slightly larger than the binodal, ϕ_B^{co}, e.g. $\phi_B^b=4.8925\times10^{-9}$, a different nucleation scenario occurs. In this case, the homogeneous mother phase is metastable and the macrophase-separated state is the thermodynamically stable one. Unlike the usual nucleation to macrophase separation, where the metastable mother phase and the stable macrophase-separated state are separated by a single maximum of the excess free energy, which is identified as the critical nucleus, the free energy of localized fluctuation structures exhibits two local maxima, ΔG_1 and ΔG_2, separated by a local minimum, ΔG_m. The structure of the nucleating droplets at the maxima and local minimum are presented in Fig. 2, which shows the density profiles of the droplet at the maxima and the local minimum for $\phi_B^b=4.8925\times10^{-9}$. At the first maximum, there is a slight enhancement of homopolymer B in the micelle core, and the droplet consists of a self-assembled micelle formed by copolymers, AB. At both, the local minimum and the second maximum, we observe that homopolymers, B, are enriched in the core of the micelle and the block copolymer, AB, is located at the interface shielding the homopolymer, B, in the interior from the A-rich mother phase. At the local minimum, the enrichment of homopolymer B is relatively weak and, therefore, the organization of block copolymer at the interface is not well developed. At the second maximum, the core is comprised of almost pure homopolymer B and a well-developed block copolymer monolayer is formed at the interface between core and mother phase. The existence of the

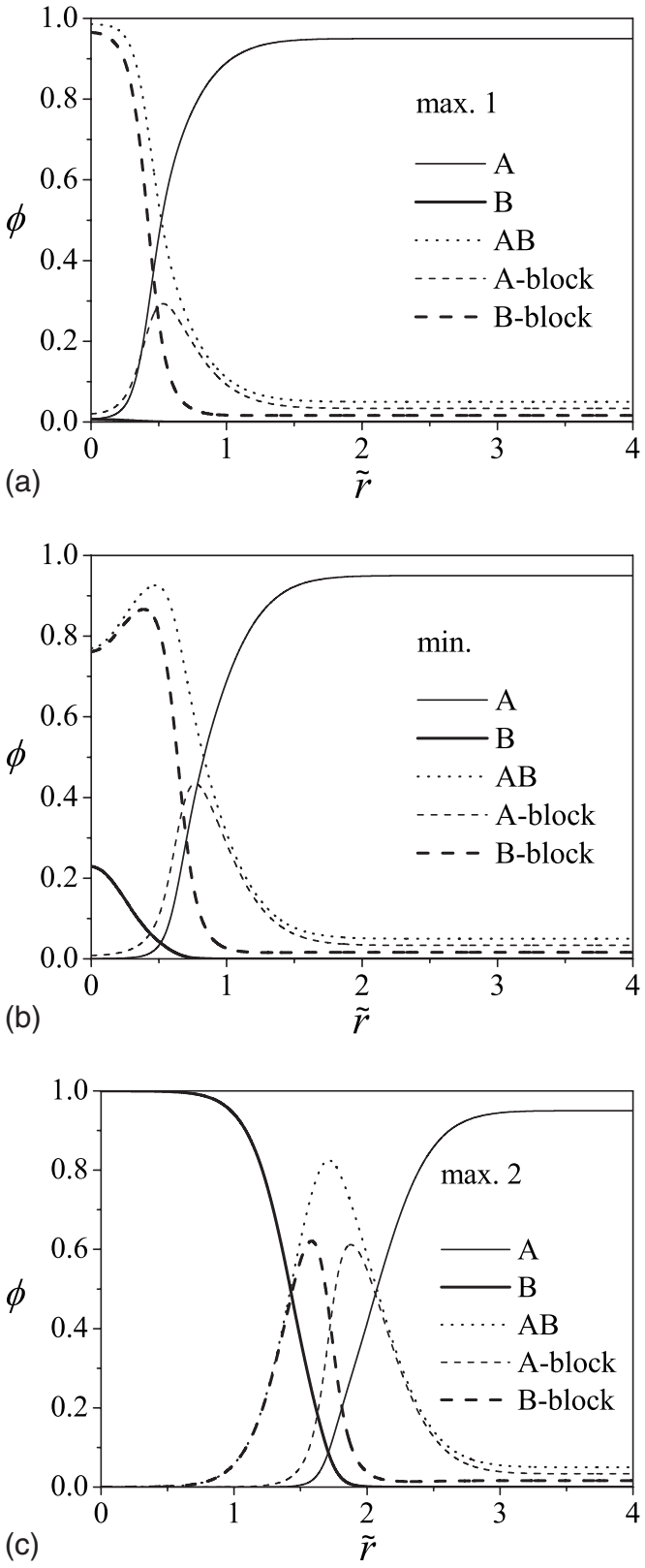

FIG. 2. Density profiles of the first critical nucleus (a), the swollen micelle (b), and the second critical nucleus (c) for a typical two-step nucleation in $A/B/AB$ bulk with $\chi N=20$, $f=0.67$, $\phi_{AB}^b=0.05$, and $\phi_B^b=4.8925\times10^{-9}$.

local minimum signals that the swollen micelle of a finite, well-defined size is metastable. Therefore, in this region, macrophase separation from the homogeneous mother phase occurs by a two-step nucleation scheme with swollen micelles as metastable intermediates. The first maximum is the critical nucleus, that characterizes the formation of micelles (or a microemulsionlike structure) from the homogeneous mother phase, and the second maximum is the critical nucleus from the micellar fluid to the thermodynamically stable macrophase-separated state. Correspondingly, we define a free energy barrier for each nucleation process: the free energy barrier for micelle formation from the mother phase is $\Delta G_{b1}=\Delta G_1$, and the free energy barrier for macrophase separation from the microemulsion amounts to $\Delta G_{b2}=\Delta G_2-\Delta G_m$. Moreover, the dissociation of the micellar fluid (or microemulsion) is also a nucleation process and its free energy barrier is the difference of grand potential between the microemulsion and the first critical nucleus, $\Delta G_{bd}=\Delta G_1-\Delta G_m$.

Upon further increasing ϕ_B^b, we find that the free energy barrier of the second step nucleation decreases and then disappears, i.e., the macrophase separation mechanism switches from a two-step nucleation to one-step one. We define the boundary between these two nucleation schemes as the microemulsion failure condition (*mfc* for concentration, ϕ_B^{mf}), beyond which microemulsion droplets of finite size cannot exist as metastable entities. For the $A/B/AB$ ternary blend at $\chi N=20$, $f=0.67$, and $\phi_{AB}^b=0.05$, this limit of metastability is $\phi_B^{\mathrm{mf}}=5.840\ 12\times10^{-9}$. In this sense, the microemulsion failure condition is the spinodal condition for macrophase separation from the micellar fluid (or microemulsion). We point out that the definition of our microemulsion failure condition is different from the emulsion failure condition in Ref. 28. Our criterion is based on the free energy variation of a single swollen micelle (or microemulsion droplet), while the latter regards the thermodynamics of the whole emulsion system.

We next examine the dependence of the maxima and the minimum of the excess free energy of forming localized, spherically symmetric fluctuation structures on ϕ_B^b. Figure 3(a) shows the excess free energy of the first critical nucleus as a function of the bulk concentration of homopolymer B. When increasing ϕ_B^b, we find that the excess free energy of the first critical nucleus decreases monotonically from a finite value at $\phi_B^b=0$ to zero at the spinodal. The decrease in ΔG_1 around and before the binodal is very small. The reason is that the first critical nucleus is driven mainly by aggregation and self-assembly of the block copolymer, and it only involves very few homopolymer B chains, especially near and before the binodal (cf. the density profile of the nucleus in Fig. 2 at $\phi_B^b=4.8925\times10^{-9}$). This point is corroborated by the behavior of the material excess of the first critical nucleus M_1 as a function of ϕ_B^b shown in Fig. 4(a). The material excess of the first critical nucleus initially decreases from a finite value, passes through a minimum, and then increases on approaching the spinodal, where is diverges. The decrease in M_1 is very small near and around the binodal of macrophase coexistence.

The excess free energy of micelle, ΔG_m, also decreases monotonically when we increase ϕ_B^b, as shown in Fig. 3(b).

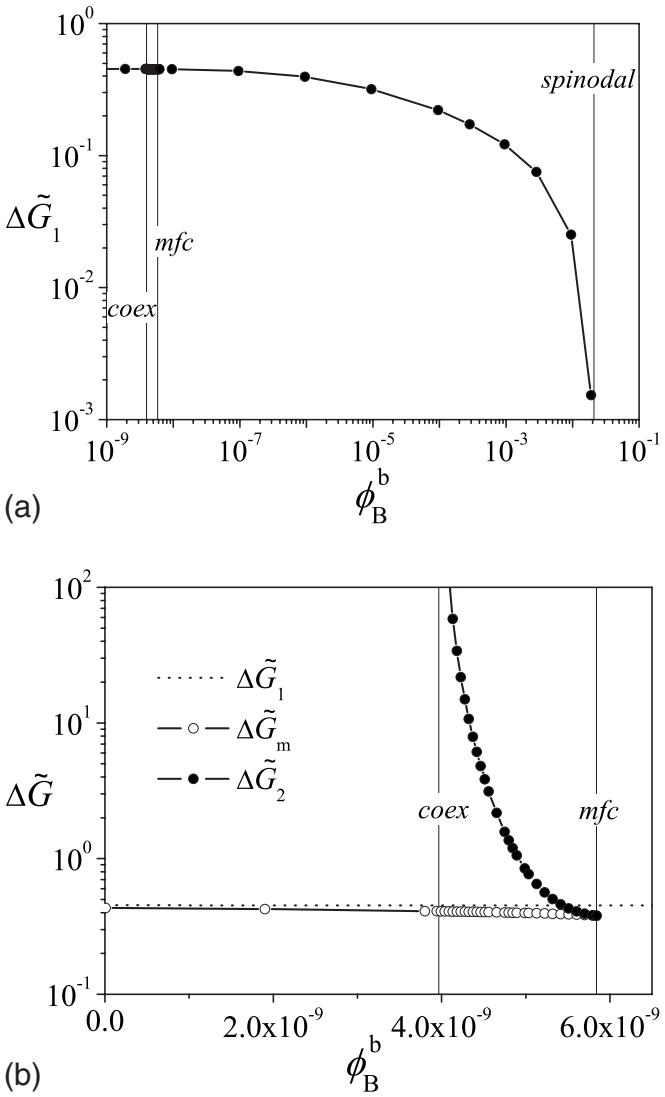

FIG. 3. Excess free energy of the first critical nucleus (a) and those of the swollen micelle and the second critical nucleus (b) as a function of the bulk concentration of homopolymer B, ϕ_B^b, at $\chi N=20$, $f=0.67$, and $\phi_{AB}^b=0.05$.

When the block copolymer concentration, ϕ_{AB}^b, is sufficient large, it is possible for ΔG_m to become negative (not shown in the figure). At the mean-field level, the condition $\Delta G_m=0$ defines the critical micelle condition (*cmc* for concentration).[42] Although some of the results we present below include cases with negative ΔG_m, we must bear in mind that when $\Delta G_m<0$, the formation of micelles becomes so favorable that they will exist in macroscopic numbers, and our assumption of isolated, noninteracting micelles no longer holds.

The excess free energy of the second critical nucleus also decreases monotonically with increasing ϕ_B^b, from infinity at the coexistence to a finite value at the *mfc*. This behavior is shown in Fig. 3(b). The decrease in the excess free energy of the second critical nucleus is faster than that of the swollen micelle and, at the *mfc*, the grand potential of the second critical nucleus equals that of the micelle. From the free energy variation, we observe that at the *mfc*, the local minimum of microemulsion and the maximum of the second critical nucleus merge into an inflexion point. The material

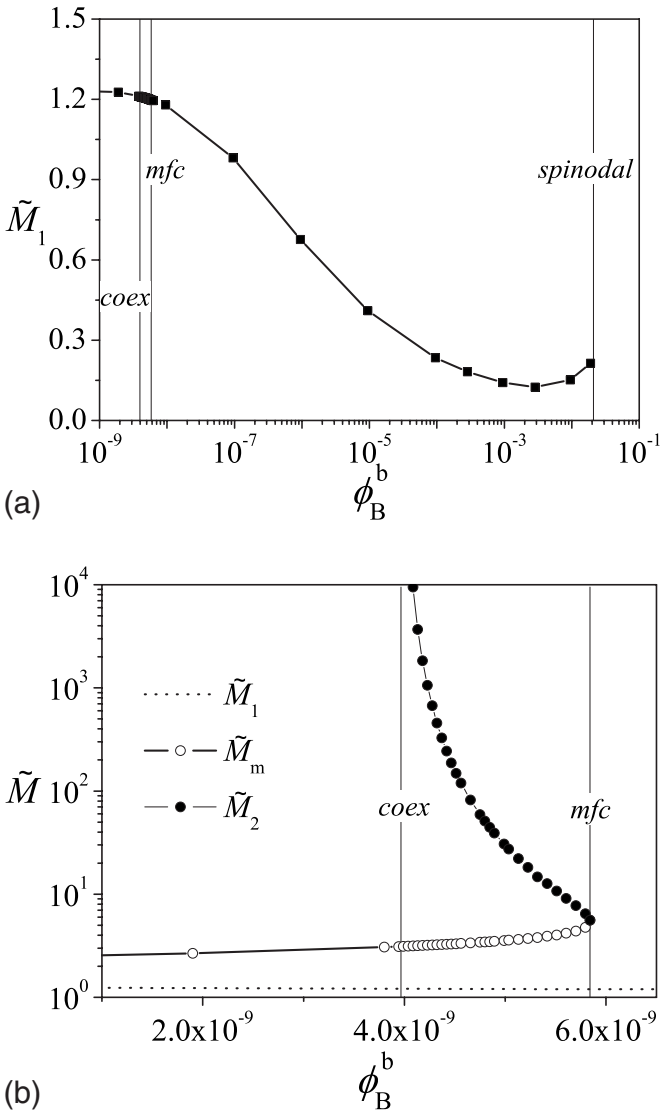

FIG. 4. Material excess of the first critical nucleus (a) and those of the swollen micelle and the second critical nucleus (b) as a function of the bulk concentration of homopolymer B, ϕ_B^b, at $\chi N=20$, $f=0.67$, and $\phi_{AB}^b=0.05$.

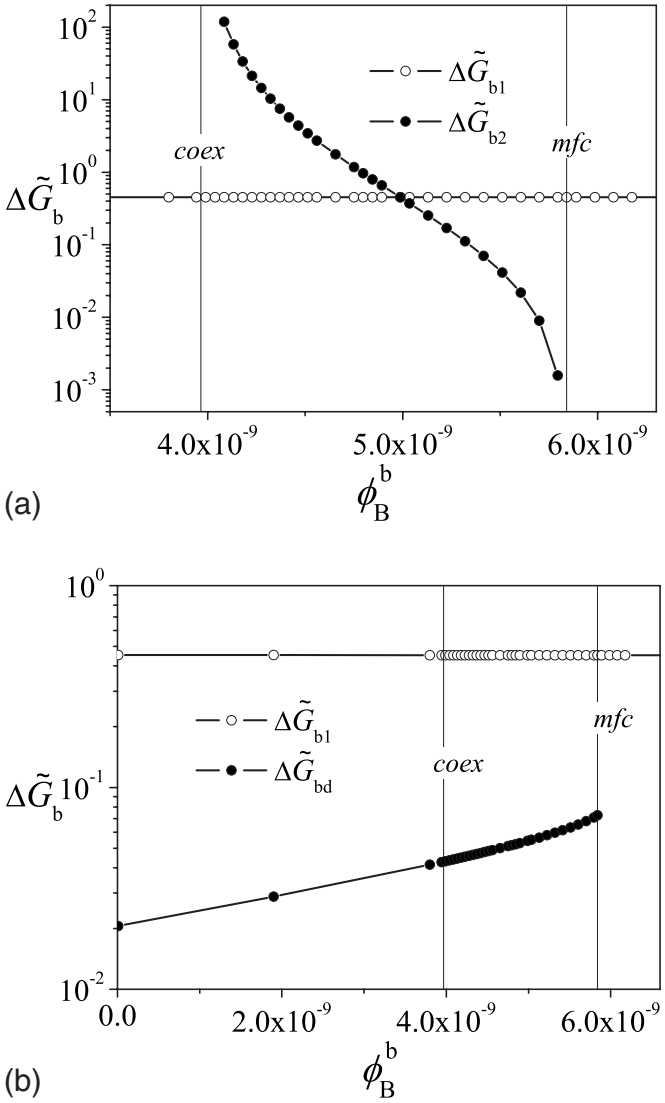

FIG. 5. Free energy barrier for the micelle formation and the sequent macrophase separation (a) and that for the micelle dissociation (b) as a function of the bulk concentration of homopolymer B, ϕ_B^b, at $\chi N=20$, $f=0.67$, and $\phi_{AB}^b=0.05$.

excess of the swollen micelle (or microemulsion droplet) and that of the second critical nucleus similarly merge at *mfc*; cf. Fig. 4(b). Increasing ϕ_B^b, the material excess of the swollen micelle increases monotonically, due to the incorporation of homopolymer, B, into the micelle. The material excess of the second critical nucleus, on the other hand, decreases monotonically from infinity at the binodal. The two quantities become equal at the *mfc*.

Studying the free energy barrier of each nucleation process provides useful insights to the dynamics of macrophase separation. Figure 5(a) shows the dependence of the free energy barriers, ΔG_{b1} and ΔG_{b2}, on the bulk density of homopolymer B. It is obvious that ΔG_{b1} remains essentially unaltered with increasing ϕ_B^b, while ΔG_{b2} decreases from infinity at the binodal to zero at the *mfc*. We can define a concentration $\phi_B^=$ where $\Delta G_{b1}=\Delta G_{b2}$. For $\phi_B^{co}<\phi_B^b\ll\phi_B^=$, the kinetics of macrophase separation from a metastable mother phase is dominated by ΔG_{b2}, whereas for $\phi_B^=\ll\phi_B^b<\phi_B^{\mathrm{mf}}$, it is dominated by ΔG_{b1}. Around $\phi_B^b\approx\phi_B^=$, both barriers, ΔG_{b1} and ΔG_{b2}, are important for the kinetics of macrophase separation. We note that although the values of the scaled free energies, $\Delta\tilde{G}_{b1}$ and $\Delta\tilde{G}_{b2}$, shown in Fig. 5 seem small, the actual value $\Delta G_b=\Delta\tilde{G}_b\sqrt{\bar{\mathcal{N}}}$ in units of kT is proportional to the square root of the molecular weight, $N^{1/2}$. Therefore, for long polymers, with a typical value of $\bar{\mathcal{N}}\sim\mathcal{O}(10^4)$, the free energy barrier ΔG_b can be quite significant.

Micelle dissociation is also a nucleation process. Figure 5(b) shows the free energy barrier for micelle formation and micelle dissociation as a function of ϕ_B^b. The free energy barrier for micelle dissociation slightly increases when increasing ϕ_B^b.

To distinguish the role of the homopolymer, B, from that of the diblock copolymer, AB, in the nucleation process, we separate the material excess along the nucleation path into a contribution from homopolymer, B, (M_B) and one from diblock copolymer, AB, (M_{AB}), as shown in Fig 6. Clearly, the first phase of nucleation is primarily the formation of a micelle due to aggregation of the diblock copolymer, AB, i.e., $M_B\simeq0$, which signals that the nucleation is initiated by

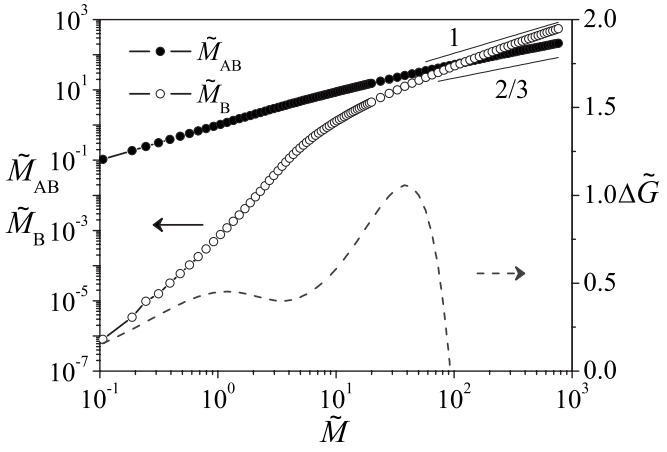

FIG. 6. Material excess of homopolymer B, M_B and diblock copolymer AB, M_{AB}, along the nucleation path for a typical two-step nucleation in an $A/B/AB$ blend at $\phi_B^b=4.8925\times10^{-9}$, $\chi N=20$, $f=0.67$, and $\phi_{AB}^b=0.05$.

the self-assembly of diblock copolymer, AB, into micelles. Thereafter, the nucleus grows into the metastable swollen micelle or the macrophase-separated state by attracting homopolymer B into the core and expanding the diblock copolymer interfacial layer. The limiting slopes on the log-log scale in the figure are consistent with the scaling of the volume and the interfacial layer. In this sense, the two-step nucleation in the $A/B/AB$ blend can be regarded as a heterogeneous nucleation. The self-assembly of AB into micelles facilitates the subsequent macrophase separation.

We have shown that a two-step nucleation to macrophase separation is possible in an $A/B/AB$ blend when the concentration of AB diblock copolymer, ϕ_{AB}^b, in the mother phase exceeds ϕ_{AB}^{md} of the A/AB blend, i.e., $\phi_{AB}^b > \phi_{AB}^{\mathrm{md}}(\phi_B^b=0)$. To complete the picture of the different phase transformation scenarios in $A/B/AB$ blends, we construct a generalized phase diagram in the $\phi_{AB}^b-\phi_B^b$ plane at $\chi N=20$, shown in Fig. 7. Five boundaries are depicted in the phase diagram:

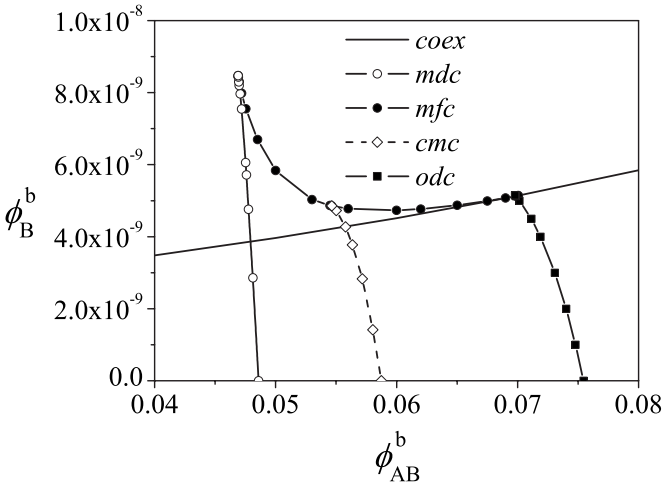

FIG. 7. A local generalized phase diagram of an $A/B/AB$ blend, marked by the coexistence of macrophase separation into A-rich and B-rich phases (*coex*, solid), the *mdc* (hollow sphere), the *mfc* (solid sphere), the *cmc* (hollow diamond), and the *odc* for periodic lamellae (solid square). In the region surrounded by the *coex*, *mdc*, and *mfc*, nucleation to macrophase separation takes place in two steps.

the A-rich binodal of macrophase separation into spatially homogenous A-rich and B-rich phases (*coex*), the *mdc*, the *mfc*, the critical microemulsion concentration (*cmc*) defined by $\Delta G_m=0$, and the *odc* concentration, where the periodic lamellae phase coexists with a uniform bulk phase. ϕ_B^b increases monotonically with an increase in ϕ_{AB}^b along the binodal of macrophase coexistence, which reflects the fact that the block copolymer AB improves the compatibility of the A/B blend. On the (*mdc*) boundary, ϕ_{AB}^b slightly decreases with an increase in ϕ_B^b, reflecting the fact that introducing a small amount of homopolymer B facilitates the formation of the metastable swollen micelles. The micelle can be metastable by virtue of the homopolymer B even when ϕ_{AB}^b is slightly smaller than $\phi_{AB}^{\mathrm{md}}(\phi_B^b=0)$. On the *mfc* curve, ϕ_B^b decreases with an increase in ϕ_{AB}^b but it increases slightly when approaching the binodal and finally merges with the coexistence. This nonmonotonic behavior can be attributed to two opposing effects of increasing ϕ_{AB}^b. On the one hand, both the excess free energy of the swollen micelle and that of the second critical nucleus decrease with increasing ϕ_{AB}^b, but the decrease in the latter is faster, which requires a lower ϕ_B^b to make the second barrier vanish. On the other hand, increasing ϕ_{AB}^b decreases the immiscibility and brings the blend close to the binodal, which increases the excess free energy of the second critical nucleus and results in a larger ϕ_B^b for the microemulsion failure. On the *cmc* boundary, ϕ_B^b decreases with an increase in ϕ_{AB}^b, indicating that the addition of homopolymer B can lower the excess free energy of micelles. Above the *cmc*, micelles have a negative excess free energy and a dense micellar fluid (i.e., microemulsion) will form. Under these conditions, the concept of a single nucleus is no longer valid. Above the *odc*, the swollen lamellar phase is stable with respect to the homogeneous bulk. Generally, the ordered phase may be comprised of periodically ordered swollen micelles. This part of the phase is included to indicate the possibility of stable, periodically ordered phases of the system, and it is not meant to be quantitatively accurate.

Both the microemulsion failure boundary and the micelle dissociation boundary terminate at their cross $(\phi_{AB}^{l1}, \phi_B^{l1})$, where the metastable swollen micelle and two critical nuclei merge into a single critical nucleus. ϕ_{AB}^{l1} characterizes the least ϕ_{AB}^b where micelles are metastable in a homogenous $A/B/AB$ blend. The microemulsion failure boundary merges with the binodal at $(\phi_{AB}^{l2}, \phi_B^{l2})$. When $\phi_{AB}^b < \phi_{AB}^{l1}$, it is impossible to form any metastable micelle even with the help of homopolymer B. When $\phi_{AB}^{\mathrm{md}}(\phi_B^0=0) > \phi_{AB}^b > \phi_{AB}^{l1}$, micelles form only with the help of some amount of homopolymer B. When $\phi_{AB}^b > \phi_{AB}^{\mathrm{md}}(\phi_B^0=0)$, micelles are formed even in the absence of homopolymer B, and adding homopolymer B swells the micelles and lowers their excess free energy. When $\phi_{AB}^b=\phi_{AB}^{l2}$, the microemulsion failure condition merges with the binodal, which means the free energy barrier for the second critical nucleus decreases from infinity to zero just at the binodal. In this case the second nucleation disappears (the droplet grows spontaneously from the swollen micelle state) and the overall free energy barrier is finite and dominated by the first critical nucleus. This situation is similar to that in the A/AB blend. Only in the region enclosed by these three boundaries, i.e., *mdc*, *mfc*, and *coex*,

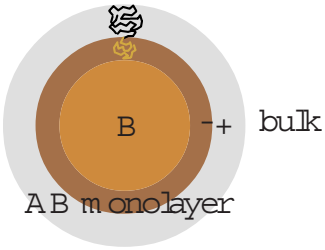

FIG. 8. (Color online) Schematic picture of a swollen micelle with a core/interface/bulk structure. The core is mainly made up of pure homopolymer B, and the interfacial is occupied by the diblock copolymer monolayer, which is approximately treated as dry brushes without any chain interpenetration of homopolymers.

does macrophase separation occur by a two-step nucleation mechanism.

B. Capillary model

Near the binodal, nucleation in A/B binary blends is well described by the classical nucleation theory, which assumes a bulklike interface between the mother phase and the nascent phase.[45] Here, we extend the capillary model to a micelle or nucleus in $A/B/AB$ blends. Fig. 8 shows the model of a droplet (swollen micelle or nucleus). A is the major component in the mother phase, B is the major component in the core of the droplet, and the block copolymer AB forms a monolayer at the interface. Assuming the grand potential density for the metastable homogeneous phase is g^b in Eq. (A8), the excess free energy of the droplet (micelle or nucleus) can be written as

$$\Delta G = \gamma A + V^c(g^c - g^b) + V^i(g^i - g^b), \tag{9}$$

where A is the interfacial area for the droplet, and V^c and V^i are the volumes for the core and the interface, respectively. The first two terms come from the usual capillary model in classical nucleation theory for A/B blends. However, the interfacial tension, γ, is the bare interfacial tension between the A and B monomers (and not the free energy cost of an A/B interface with adsorbed diblock copolymers) and, therefore, it is always positive. g^c is the grand potential density for the core (with composition ϕ_A^c, ϕ_B^c and ϕ_{AB}^c), and can be calculated from its Helmholtz free energy density, f^c, as $g^c = f^c - \mu_A^b \phi_A^c - \mu_B^b \phi_B^c$, with μ_A^b and μ_B^b as the chemical potentials in the metastable mother phase. $g^c - g^b$ is the grand potential density difference between the inside and the outside of the droplet. For A/B blends, $g^c - g^b > 0$ when the system is in single-phase region and $g^c - g^b < 0$ when the system is supersaturated. The sum of the third term and the first term is the net contribution of the interface, and g^i is the grand potential density for the interfacial monolayer due to chain stretching of the block copolymers in the micelle or microemulsion droplet. To be consistent with the numerical SCFT, ΔG, γ, g, and g^b have been divided by k_BT in Eq. (9).

In the strong segregation regime, it is reasonable to assume that the core phase is almost pure B, and the interfacial layer is occupied by diblock copolymer monolayer. Therefore, the work of formation can be expressed as

$$\Delta G = \gamma A + n_B^c Nv(g^c - g^b) + n_{AB}^i Nv(g^i - g^b), \tag{10}$$

where n_B^c is the number of homopolymer B in the core and n_{AB}^i is the number of diblock copolymer in the interfacial layer. From the sketched geometry, we obtain $A = \sqrt[3]{36\pi}[n_B^c Nv + n_{AB}^i(1-f)Nv]^{2/3}$. The core phase has $Nvg^c = -1 - \mu_B^b$ using the free energy shown in Eq. (A9) and setting $\phi_B = 1$ and $\phi_A = \phi_{CD} = 0$. The diblock copolymer monolayer at the interface can be considered as dry polymer brushes on either side of the dividing surface and its grand potential per chain is given by[50,51]

$$Nvg^i = \ln\left(a\frac{n_{AB}^i}{A}\right) + N_+ vg_+^i + N_- vg_-^i, \tag{11}$$

where $N_+ = fN$ and $N_- = (1-f)N$, the first term is the translational entropy of the grafting points at the interface, where a is the area of a grafting point. The last two terms are the elastic free energy of the brush at the concave (denoted by subscript $-$) and convex (denoted by subscript $+$) side of the interface. Both quantities are functions of the grafting density. The translational entropy of the grafting points can usually be neglected. According to Ref. 51, we find

$$N_\pm vg_\pm^i = \frac{\pi^2 h_\pm^2}{16N_\pm b^2}\frac{1 + \frac{3}{2}H_\pm h_\pm + \frac{3}{5}Kh_\pm^2}{1 + H_\pm h_\pm + \frac{1}{3}Kh_\pm^2}, \tag{12}$$

where h is the brush height, and H and K are mean curvature and Gaussian curvature of the interface, respectively. From the geometry shown in Fig. 8, we have $K = 4\pi/A$ and $H_\pm = \pm 2\sqrt{\pi/A}$. The brush heights can be determined from the incompressibility conditions,

$$\frac{1}{3}Kh_\pm^3 + H_\pm h_\pm^2 + h_\pm = N_\pm v\frac{n_{AB}^i}{A}. \tag{13}$$

From Eqs. (10)–(13), we thus obtain the excess free energy of the droplet (nucleus or micelle) as a function of n_B^c and n_{AB}^i. The droplet can be described by n_B^c and n_{AB}^i. To relate this schematic model to the results of SCFT, we write $M_B^c \simeq n_B^c Nv$, $M_{AB}^i \simeq n_{AB}^i Nv$ and $M \simeq n_B^c Nv + n_{AB}^i Nv$, and the excess free energy becomes

$$\Delta G = \gamma A + M_B^c(g^c - g^b) + M_{AB}^i(g^i - g^b), \tag{14}$$

which can be rewritten in a dimensionless form

$$\Delta\tilde{G} = \tilde{\gamma}\tilde{A} + \tilde{M}_B^c(\tilde{g}^c - \tilde{g}^b) + \tilde{M}_{AB}^i(\tilde{g}^i - \tilde{g}^b) \tag{15}$$

using the rescaled, dimensionless quantities in Eq. (8) along with $\tilde{A} \equiv A/R_e^2$ and $\tilde{\gamma} \equiv \gamma R_e^2/\sqrt{\bar{N}}$.

$\tilde{g}^b$ and $\tilde{g}^c$ are calculated from the specified mother phase. In principle, $\tilde{\gamma}$ can be determined numerically from the equilibrium planar interface by SCFT calculations.[45] However, the focus of this section is to obtain a simplified picture of the system, and numerical accuracy is not our main concern. Therefore, to get the right order of magnitude, we adjust $\tilde{\gamma}$ such that we have the same ϕ_{AB}^{md} for A/AB capillary model as that in SCFT. For example, at $f = 0.67$ and $\chi N = 20$, we have $\phi_{AB}^{md} = 0.0486$, and thus we choose $\tilde{\gamma} = 1.867\,213$, which is very close to the prediction in the strong segregation limit, $\tilde{\gamma}_{SSL} = \sqrt{\chi N/6} = 1.826$.

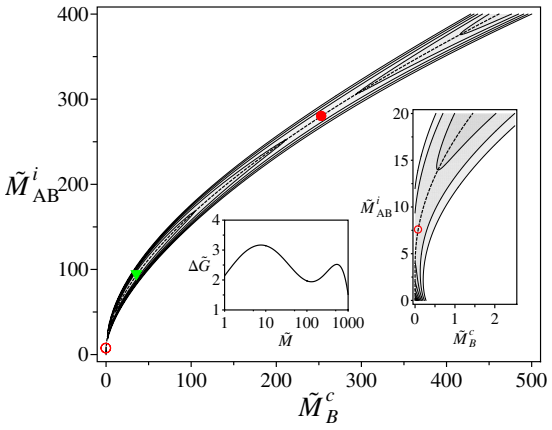

FIG. 9. (Color online) Contour plot of the excess free energy of the nascent droplet (nucleus and micelle) on the parameter plane of M^c_B and M^i_{AB} for an $A/B/AB$ blend with $f=0.67$, $\chi N=20$, $\phi^b_{AB}=0.0455$, $\phi^b_B=3.916\ 313\ 5\times10^{-9}$, and $\tilde{\gamma}=1.867\ 213$, along with the optimum kinetic path marked by a thick dashed line. The selection of gray-scale scheme makes regions of high value of excess free energy white and only regions near the optimum kinetic path distinguishable. The first critical nucleus is marked by hollow sphere symbol, the second critical nucleus by solid sphere symbol and microemulsion by triangle symbol. The left inset shows the excess free energy as function of the total material excess along the optimum kinetic path and the right inset is a magnified picture of local section near $M^c_B=0$ and $M^i_{AB}=0$.

Now we examine the excess free energy of the newly formed droplet as a function of $\tilde{M}^c_B$ and $\tilde{M}^i_{AB}$. Figure 9 shows the free energy landscape near the nucleation path in the form of a contour plot. The parameters are $f=0.67$, $\chi N=20$, $\phi^b_{AB}=0.0455$, and $\phi^b_B=3.916\ 313\ 5\times10^{-9}$. The nucleation path is shown by the dash line. When the free energy is plotted as a function of the total material excess $\tilde{M}=\tilde{M}^c_B+\tilde{M}^i_{AB}$ along the nucleation path, we obtain a free energy plot shown in the inset of Fig. 9, which is similar to the one shown in Fig. 1 from the SCFT calculation. For these conditions, we clearly observe a two-step nucleation to macrophase separation with swollen micelles as an intermediate.

Zooming in on the region of small $\tilde{M}^c_B$ and $\tilde{M}^i_{AB}$, we see how the system surpasses the first free energy barrier. It is clear that the first nucleation primarily involves the self-assembly of AB diblock copolymers, which is consistent with the results from SCFT. On the other hand, a small amount of homopolymer B helps to stabilize micelle. For the case $\phi^b_{AB}=0.0455<\phi^{\rm md}_{AB}=0.0486$ shown in Fig. 9, it is impossible to have metastable micelles without homopolymer B (see the excess free energy at $\tilde{M}^c_B=0$), but adding some amount of homopolymer B into nucleus of AB decreases its free energy and leads to metastable micelles. Even for the case $\phi^b_{AB}=0.067>\phi^{\rm md}_{AB}=0.0486$ (not shown here), where the micelle can form without help of homopolymer, B, the free energy of micelles can be lowered by adding a small amount of homopolymer, B.

We end this section by briefly commenting on the validity of the assumption in our extended capillary model. We assume the nucleus or swollen micelle has a core-interfacial layer-bulk structure, where the core is comprised of pure homopolymer, B, and the interfacial layer is a pure block copolymer monolayer. To calculate the free energy contribution of the diblock copolymer monolayer, we also assume there is no chain interpenetration between homopolymer and block copolymer layer, and no interfacial energy at the boundary between the AB monolayer and the core or the bulk. While the former assumption is only true at very strong segregation, the neglect of the interfacial tension between the dry brush formed by the monolayer and the respective homopolymer-rich regions is only permissible at intermediate segregation.[42] At the segregation considered here, both assumptions are reasonably good approximations but we do not expect quantitative agreement between the results of the extended capillary model and those from the numerical SCFT. Despite its crudeness, however, our extended capillary model captures the key features of the phenomena.

IV. CONCLUSIONS

Using the numerical SCFT, we examine the nucleation in $A/B/AB$ ternary polymer blends, with a focus on the thermodynamic relationship between swollen micelles (or microemulsions) and macrophase separation. Due to the interplay between micellar self-assembly of diblock copolymers, AB, and macrophase separation of the A/B blend, we find a two-step nucleation process toward macrophase separation with microemulsion droplets of finite size as metastable intermediates. The results from numerical SCFT calculation are qualitatively corroborated by an extended capillary model, where the free energy contribution of the diblock copolymer monolayer at the interface is given by the dry brush model. Our results support the proposition that a two-step nucleation mechanism is a common feature of systems with short-range attraction and long-range repulsion, although only in a small part of the phase diagram. It will be interesting to examine the full parameter space to see how this regime of the phase diagram can be enlarged. We hope this two-step nucleation to macrophase separation and its influence on phase separation dynamics will be studied by future experiments.

The full phase behavior of $A/B/AB$ ternary systems is extremely rich and complex, and our study is limited to systems that macrophase separate into A-rich and B-rich phases. From the free energy behavior of the growing nucleus, we identify the micelle dissociation condition where, on graphs that depict the dependence of the excess free energy of the nucleus on the material excess, the first critical nucleus and swollen micelle merge into an inflexion point, and the microemulsion failure condition where the swollen micelle and the second critical nucleus merge into an inflexion point. On the density plane $\phi^b_B-\phi^b_{AB}$, the two-step nucleation occurs in a region enclosed by the binodal, the micelle dissociation boundary and the microemulsion failure boundary.

Introducing small amount of homopolymer B into a micelle-forming A/AB blend aids in forming micelle as well as in decreasing the free energy barrier between the swollen micelle and the macrophase-separated state. Only when ϕ^b_{AB} is above its micelle dissociation value, can micelles or microemulsions form. Increasing ϕ^b_{AB} leads to a decrease in the excess free energy of micelles, which stabilizes the swollen micelles; but under some conditions, adding more diblock

copolymer AB can lead to a microemulsion failure because the decrease in ΔG of the second critical nucleus can be faster than that of micelles.

Compared to the simple $A/B/AB$ blend, $A/B/CD$ blends have much more complex phase behavior and the vast parameter space allows for structures that are difficult to obtain in the $A/B/AB$ blend. Experiments and theories have shown that in $A/B/AC$, it is easier to balance the amphiphilic interaction to microemulsions by adjusting χ_{AC} and χ_{BC}.[13–19] Thus, it will be interesting to study nucleation in the $A/B/AC$ and $A/B/CD$ blends.

In this study, only fluctuations of spherically symmetry are considered. As the referee suggested, if the constraint of symmetry is released, it is possible that the nucleation mechanism can be altered. However, the two-step nucleation scheme revealed here is still nontrivial. Further study on fluctuations of other shapes will help to fully understand phase behavior in $A/B/CD$ blends.

ACKNOWLEDGMENTS

Financial support by the DFG within the Materials World Network (Grant No. Mu 1674/4) is gratefully acknowledged. This work is also partially supported by the National Natural Science Foundation of China (Grant No. 20620120105) Programs.

APPENDIX: SCFT SOLUTION FOR A HOMOGENEOUS PHASE

The homogeneous bulk state is always a solution to the self-consistent field equation. For the homogeneous mixture with $\{\phi_j^b\}$, the self-consistent field equations can be solved to get ξ^b, $\{\omega_j^b\}$, and $\{\mu_\alpha^b\}$. For the following derivation, homogeneity is understood, and to keep concise the superscript b is ignored. The molecular field can be calculated as

$$v\xi = -\frac{\ln \phi_{CD}}{N_{CD}} - [f\chi_{AC} + (1-f)\chi_{AD}]\phi_A - [f\chi_{BC} + (1-f)\chi_{BD}]\phi_B - 2\chi_{CD}f(1-f)\phi_{CD}, \tag{A1}$$

$$v\omega_A = -\frac{\ln \phi_{CD}}{N_{CD}} - [f\chi_{AC} + (1-f)\chi_{AD}]\phi_A - [f\chi_{BC} + (1-f)\chi_{BD} - \chi_{AB}]\phi_B - [2f(1-f)\chi_{CD} - f\chi_{AC} - (1-f)\chi_{AD}]\phi_{CD}, \tag{A2}$$

$$v\omega_B = -\frac{\ln \phi_{CD}}{N_{CD}} - [f\chi_{AC} + (1-f)\chi_{AD} - \chi_{AB}]\phi_A - [f\chi_{BC} + (1-f)\chi_{BD}]\phi_B - [2f(1-f)\chi_{CD} - f\chi_{BC} - (1-f)\chi_{BD}]\phi_{CD}, \tag{A3}$$

$$v\omega_C = -\frac{\ln \phi_{CD}}{N_{CD}} - (1-f)(\chi_{AD} - \chi_{AC})\phi_A - (1-f)(\chi_{BD} - \chi_{BC})\phi_B - (2f-1)(1-f)\chi_{CD}\phi_{CD}, \tag{A4}$$

$$v\omega_D = -\frac{\ln \phi_{CD}}{N_{CD}} - f(\chi_{AC} - \chi_{AD})\phi_A - f(\chi_{BC} - \chi_{BD})\phi_B - (1-2f)f\chi_{CD}\phi_{CD}, \tag{A5}$$

and the chemical potential can be written as

$$v\mu_A = \frac{\ln \phi_A}{N_A} - \frac{\ln \phi_{CD}}{N_{CD}} - [f\chi_{AC} + (1-f)\chi_{AD}]\phi_A - [f\chi_{BC} + (1-f)\chi_{BD} - \chi_{AB}]\phi_B - [2f(1-f)\chi_{CD} - f\chi_{AC} - (1-f)\chi_{AD}]\phi_{CD}, \tag{A6}$$

$$v\mu_B = \frac{\ln \phi_B}{N_B} - \frac{\ln \phi_{CD}}{N_{CD}} - [f\chi_{AC} + (1-f)\chi_{AD} - \chi_{AB}]\phi_A - [f\chi_{BC} + (1-f)\chi_{BD}]\phi_B - [2f(1-f)\chi_{CD} - f\chi_{BC} - (1-f)\chi_{BD}]\phi_{CD}. \tag{A7}$$

Therefore, the grand potential density (rescaled by v) is

$$vg = \frac{\ln \phi_{CD}}{N_{CD}} + [f\chi_{AC} + (1-f)\chi_{AD}]\phi_A + [f\chi_{BC} + (1-f)\chi_{BD}]\phi_B + 2f(1-f)\chi_{CD}\phi_{CD} - \frac{1}{2}\sum_{jj'}\chi_{jj'}\phi_j\phi_{j'} - \frac{\phi_A}{N_A} - \frac{\phi_B}{N_B} - \frac{\phi_{CD}}{N_{CD}}, \tag{A8}$$

and the Helmholtz free energy density is

$$vf = \frac{\phi_B(\ln \phi_B - 1)}{N_B} + \frac{\phi_A(\ln \phi_A - 1)}{N_A} + \frac{\phi_{CD}(\ln \phi_{CD} - 1)}{N_{CD}} + \chi_{AB}\phi_A\phi_B + [f\chi_{AC} + (1-f)\chi_{AD}]\phi_A\phi_{CD} + [f\chi_{BC} + (1-f)\chi_{BD}]\phi_B\phi_{CD} + f(1-f)\chi_{CD}\phi_{CD}^2. \tag{A9}$$

The free energy density of mixing Δf_{mix} is given by

$$v\Delta f_{\mathrm{mix}} = \frac{\phi_B \ln \phi_B}{N_B} + \frac{\phi_A \ln \phi_A}{N_A} + \frac{\phi_{CD}\ln \phi_{CD}}{N_{CD}} + [f\chi_{AC} + (1-f)\chi_{AD}]\phi_A\phi_{CD} + [f\chi_{BC} + (1-f)\chi_{BD}]\phi_B\phi_{CD} + \chi_{AB}\phi_A\phi_B. \tag{A10}$$

In order to specify the thermodynamic state of the homogenous phase, we need to know the phase diagram for the ternary system. The full phase diagram for the $A/B/CD$ ternary blend is quite complex.[5–28] In this work, we are interested in systems that exhibits phase coexistence between macroscopic A-rich and B-rich phases. For a given overall composition, the coexistence between the A-rich and B-rich phases is determined by the equality of the grand potential and the chemical potential of species of homopolymers A and B, respectively, in both phases, and the equality of the grand potential of the two phases. In general these conditions lead to a set of transcendental equations that can only be solved numerically. The spinodal curve (the limit of instability of the homogeneous phase) is determined by[52]

$$\begin{vmatrix} f_{AA} & f_{AB} \\ f_{BA} & f_{BB} \end{vmatrix} = 0, \tag{A11}$$

with

$$f_{IJ} = \left(\frac{\partial}{\partial \phi_I} - \frac{\partial}{\partial \phi_{CD}}\right)\left(\frac{\partial}{\partial \phi_J} - \frac{\partial}{\partial \phi_{CD}}\right)\Delta f_{\mathrm{mix}},$$

$$I,J = A,B, \tag{A12}$$

[1] K. Mittal and P. Bothorel, *Surfactants in Solution* (Plenum, New York, 1986).
[2] M. Kahlweit and R. Strey, Angew. Chem., Int. Ed. Engl. **24**, 654 (1985).
[3] R. Strey, Colloid Polym. Sci. **272**, 1005 (1994).
[4] S. H. Chen and S. Choi, Supramol. Sci. **5**, 197 (1998).
[5] D. Broseta and G. H. Fredrickson, J. Chem. Phys. **93**, 2927 (1990).
[6] R. Holyst and M. Schick, J. Chem. Phys. **96**, 7728 (1992).
[7] W. C. Hu, J. T. Koberstein, J. P. Lingelser, and Y. Gallot, Macromolecules **28**, 5209 (1995).
[8] S. T. Milner and H. W. Xi, J. Rheol. **40**, 663 (1996).
[9] R. A. L. Jones, Curr. Opin. Solid State Mater. Sci. **2**, 673 (1997).
[10] L. Kielhorn and M. Muthukumar, J. Chem. Phys. **107**, 5588 (1997).
[11] P. K. Janert and M. Schick, Macromolecules **30**, 137 (1997).
[12] R. B. Thompson and M. W. Matsen, J. Chem. Phys. **112**, 6863 (2000).
[13] J. H. Lee, N. P. Balsara, R. Krishnamoorti, H. S. Jeon, and B. Hammouda, Macromolecules **34**, 6557 (2001).
[14] J. H. Lee, M. L. Ruegg, N. P. Balsara, Y. Q. Zhu, S. P. Gido, R. Krishnamoorti, and M. H. Kim, Macromolecules **36**, 6537 (2003).
[15] B. J. Reynolds, M. L. Ruegg, N. P. Balsara, C. J. Radke, T. D. Shaffer, M. Y. Lin, K. R. Shull, and D. J. Lohse, Macromolecules **37**, 7401 (2004).
[16] M. L. Ruegg, B. J. Reynolds, M. Y. Lin, D. J. Lohse, and N. P. Balsara, Macromolecules **39**, 1125 (2006).
[17] M. L. Ruegg, B. J. Reynolds, M. Y. Lin, D. J. Lohse, and N. P. Balsara, Macromolecules **40**, 1207 (2007).
[18] M. D. Lefebvre and K. R. Shull, Macromolecules **39**, 3450 (2006).
[19] M. L. Nunalee, H. X. Guo, M. O. de la Cruz, and K. R. Shull, Macromolecules **40**, 4721 (2007).
[20] M. Müller and M. Schick, J. Chem. Phys. **105**, 8885 (1996).
[21] A. Werner, F. Schmid, K. Binder, and M. Mueller, Macromolecules **29**, 8241 (1996).
[22] H. S. Jeon, J. H. Lee, N. P. Balsara, and M. C. Newstein, Macromolecules **31**, 3340 (1998).
[23] F. S. Bates, W. W. Mauerer, T. P. Lodge, M. F. Schulz, M. W. Matsen, K. Almdal, and K. Mortensen, Phys. Rev. Lett. **75**, 4429 (1995).
[24] F. S. Bates, W. W. Maurer, P. M. Lipic, M. A. Hillmyer, K. Almdal, K. Mortensen, G. H. Fredrickson, and T. P. Lodge, Phys. Rev. Lett. **79**, 849 (1997).
[25] M. A. Hillmyer, W. W. Maurer, T. P. Lodge, F. S. Bates, and K. Almdal, J. Phys. Chem. B **103**, 4814 (1999).
[26] N. R. Washburn, T. P. Lodge, and F. S. Bates, J. Phys. Chem. B **104**, 6987 (2000).
[27] L. Leibler, Makromol. Chem., Macromol. Symp. **16**, 1 (1988).
[28] Z.-G. Wang and S. A. Safran, J. Phys. (Paris) **51**, 185 (1990).
[29] L. Leibler, Macromolecules **13**, 1602 (1980).
[30] T. Ohta and K. Kawasaki, Macromolecules **19**, 2621 (1986).
[31] M. W. Matsen and F. S. Bates, Macromolecules **29**, 1091 (1996).
[32] F. S. Bates and G. H. Fredrickson, Phys. Today **52**(2), 32 (1999).
[33] X. H. He and F. Schmid, Phys. Rev. Lett. **100**, 137802 (2008).
[34] J. Wang, H. Zhang, F. Qiu, Z.-G. Wang, and Y. Yang, J. Chem. Phys. **118**, 8997 (2003).
[35] N. P. Balsara, C. Lin, and B. Hammouda, Phys. Rev. Lett. **77**, 3847 (1996).
[36] A. A. Lefebvre, J. H. Lee, H. S. Jeon, N. P. Balsara, and B. Hammouda, J. Chem. Phys. **111**, 6082 (1999).
[37] N. A. M. Besseling and M. A. Cohen Stuart, J. Chem. Phys. **110**, 5432 (1999).
[38] V. Talanquer and D. W. Oxtoby, J. Chem. Phys. **113**, 7013 (2000).
[39] M. Monzen, T. Kawakatsu, M. Doi, and R. Hasegawa, Comput. Theor. Polym. Sci. **10**, 275 (2000).
[40] D. Duque, J. Chem. Phys. **119**, 5701 (2003).
[41] J. Wang, Z.-G. Wang, and Y. Yang, Macromolecules **38**, 1979 (2005).
[42] A. Cavallo, M. Müller, and K. Binder, Macromolecules **39**, 9539 (2006).
[43] S. B. Hutchens and Z.-G. Wang, J. Chem. Phys. **127**, 084912 (2007).
[44] T. Ohta, M. Motoyama, and A. Ito, J. Phys.: Condens. Matter **8**, A65 (1996).
[45] S. M. Wood and Z.-G. Wang, J. Chem. Phys. **116**, 2289 (2002).
[46] M. Müller, L. G. MacDowell, P. Virnau, and K. Binder, J. Chem. Phys. **117**, 5480 (2002).
[47] K. H. Dai, E. J. Kramer, and K. R. Shull, Macromolecules **25**, 220 (1992).
[48] K. R. Shull, Macromolecules **26**, 2346 (1993).
[49] I. Kusaka, Z.-G. Wang, and J. H. Seinfeld, J. Chem. Phys. **108**, 3416 (1998).
[50] Z.-G. Wang and S. A. Safran, J. Chem. Phys. **94**, 679 (1991).
[51] S. P. Gido and Z.-G. Wang, Macromolecules **30**, 6771 (1997).
[52] C. Huang, M. Olvera de la Cruz, and B. W. Swift, Macromolecules **28**, 7996 (1995).